Scripta Materialia 177 (2020) 218–222

Contents lists available at ScienceDirect

Scripta Materialia

journal homepage: www.elsevier.com/locate/scriptamat

Calculating the magnetocaloric effect in second-order-type material by micromagnetic simulations: A case study on Co_2B

Dominik Ohmer[a,*], Min Yi[a,b,c], Maximilian Fries[a], Oliver Gutfleisch[a], Bai-Xiang Xu[a]

[a] Institute of Materials Science, Technische Universität Darmstadt, Darmstadt 64287, Germany
[b] State Key Lab of Mechanics and Control of Mechanical Structures & Key Lab for Intelligent Nano Materials and Devices of Ministry of Education & College of Aerospace Engineering, Nanjing University of Aeronautics and Astronautics (NUAA), Nanjing 210016, China
[c] State Key Lab for Strength and Vibration of Mechanical Structure, Xi'an Jiaotong University, Xi'an 710049, China

ARTICLE INFO

Article history:
Received 5 September 2019
Revised 17 October 2019
Accepted 24 October 2019
Available online 4 November 2019

Keywords:
Magnetocaloric effect
Micromagnetic simulation
Arrott–Noakes equation
Microstructure
Entropy change

ABSTRACT

We propose a calculation scheme which integrates micromagnetic simulations and the Arrott–Noakes equation for the investigation of the influence of microstructure and magnetocrystalline anisotropy on the magnetocaloric effect (MCE) in second-order magnetic phase transition materials. Using the Arrott–Noakes equation, the micromagnetic simulation results are extrapolated to temperatures above Curie temperature and applied to MCE calculations. With Co_2B as model material, we found that increasing magnetocrystalline anisotropy facilitates higher isothermal entropy changes (ΔS_T). The grain size reduction results in increased ΔS_T for constant saturation magnetization (M_S), while ΔS_T decreases for a reduction of M_S with reduced grain size.

As the global energy consumption, especially for cooling, is expected to increase, the research for more energy efficient cooling devices is of high interest. Magnetic cooling devices show Carnot efficiencies of up to 60% and are therefore considered as a promising alternative to conventional gas compression cooling devices. [1–3] Besides higher efficiency, magnetic cooling devices are free of refrigerant gases. Since the discovery of the giant magnetocaloric effect (MCE), [4] several promising material systems, e.g., La–Fe–Si–, [5–8] Fe_2P-based, [9–12] and Heusler alloys, [13,14] have been studied extensively for potential application in MCE refrigeration. [15] In these systems, MCE properties, such as the isothermal entropy change ΔS_T and adiabatic temperature change ΔT_{ad}, are tunable by elemental substitutions.

However, there are other properties that can affect the MCE of a material system. Liu et al. [16] reported about the influence of the annealing process, i.e., the microstructure, on the transition temperature and hysteresis in La–Fe–Si alloys. Gottschall et al. [17] showed a sharpening of the phase transition in the first-order phase transition (FOPT) materials with decreasing grain size. Fries et al. [18] recently investigated the effect of magnetocrystalline anisotropy on the MCE in Co_2B.

Modeling of the MCE is of high interest, as a systematic experimental study of the relation between microstructure, magnetocrystalline anisotropy, and the MCE would include complex synthesis routes and annealing processes. There are different approaches for modeling the MCE. For FOPT materials first-principle calculations [19–21] are used to obtain exchange coupling energies and magnetic moments, which are inserted in thermomagnetic models like the Bean–Rodbell [22] model. Thermodynamic models, which describe the system by a set of macroscopic variables, can be used for FOPT [23,24] and for second-order phase transition (SOPT) [25–27] materials. The Arrott–Noakes equation (ANE) is an equation of state widely used for SOPT materials. [28] However, the above mentioned models cannot account for the microstructure. Magnetic microstructures can be taken into account in micromagnetic simulations. [29–31] They are based on the Landau–Lifshitz–Gilbert (LLG) equation and take the magnetocrystalline anisotropy K, the exchange constant A, and the saturation magnetization M_S as input parameters. But as M_S is zero above T_C, micromagnetic simulations are generally limited to temperatures below T_C.

In this work, we combine now micromagnetic simulations with the ANE for investigating the influence of microstructure and magnetocrystalline anisotropy on the MCE in Co_2B nanograins in the size range of 5 to 100 nm. In doing so, we can vary the grain size, boundary thickness, and anisotropy constant K and calculate ΔS_T. In detail, we propose three steps for the calculation of ΔS_T. Firstly, micromagnetic simulations with varied microstructures and

* Corresponding author.
E-mail addresses: dohmer@mfm.tu-darmstadt.de (D. Ohmer), yimin@nuaa.edu.cn (M. Yi).

https://doi.org/10.1016/j.scriptamat.2019.10.039
1359-6462/

magnetocrystalline anisotropy are performed for temperatures up to T_C. Secondly, the magnetization curves from the micromagnetic simulations are used to determine the parameters of ANE. Finally, the parameterized ANE is used to calculate ΔS_T according to the Maxwell relations. [32]

The ANE is an equation of state, which phenomenologically describes the temperature and field dependence of the magnetization of SOPT materials in the vicinity of T_C. In the ANE, the magnetization is described by

$$\left(\frac{H}{M}\right)^{\frac{1}{\gamma}} = a(T - T_C) + bM^{\frac{1}{\beta}}, \tag{1}$$

with a and b as characteristic constants for the material under study. The critical exponents β and γ can be obtained through the Kouvel–Fisher method [33] which is based on the equations

$$M_0(T) \cdot \left[\frac{dM_0(T)}{dT}\right]^{-1} = \frac{T - T_C}{\beta}, \tag{2}$$

$$\chi_0^{-1}(T) \cdot \left[\frac{d\chi_0^{-1}(T)}{dT}\right]^{-1} = \frac{T - T_C}{\gamma}. \tag{3}$$

The spontaneous magnetization M_0 and initial susceptibility χ_0 can be determined by linearly fitting the Arrott plots ($M^{2.5}$ *vs.* $(H/M)^{0.75}$). Since micromagnetic simulations only work below T_C, the direct fitting of the ANE by using micromagnetic results produces unreasonable results. To overcome this problem, we make use of the experimental data. More specifically, as a and b are material-specific, we make the assumption that they do not strongly depend on microstructure, and determine a and b by using the experimental data. The microstructure-related β and γ can be obtained by using the micromagnetic results and the aforementioned Kouvel–Fisher method. As a proof of concept of the proposed methodology, we take a typical SOPT material (Co_2B) as the model material.

Applying the Kouvel–Fisher method to the results from Fries et al. [18] and creating the corresponding Arrott plots (see Fig. 1 in supplementary), we determine β and γ to be 0.307 and 1.118, respectively. According to literature, the values for β and γ should be in the range of 0.4 and 4/3, respectively. The value 4/3 corresponds to the solution for the three-dimensional Heisenberg model, [34] while 5/4 corresponds to the solution for the Ising model. [35] If γ is closer to 5/4 or 4/3 than to the unity, it would imply short-range correlations in the spin-orientation, which are not considered in the molecular field model. [33] Using the obtained β and γ, we fit the experimental data with the ANE and get $a = 0.379$ and $b = 2.07 \cdot 10^{-17}$. With all four parameters obtained, we plot the ANE in comparison with the experimental data (see Fig. 2 in supplementary). Our results agree well with the experimental data in Ref. [18] so that we will use the obtained a and b values to investigate the influence of microstructure and K on the MCE of Co_2B nanograins.

Micromagnetic simulations are performed using the Object Oriented MicroMagnetic Framework (OOMMF). [36] We create the model geometry with a microstructure composed of $4 \times 4 \times 4$ cube-shaped Co_2B grains and straight grain boundaries. The grain sizes range from 5 to 100 nm, while the grain boundary thicknesses range from 0 to 10 nm. In all cases the mesh size is set as 2 nm. The grain boundaries are assumed to be non-magnetic. The saturation magnetization (M_0) and magnetocrystalline anisotropy (K) of Co_2B strongly depend on temperature and are taken from the measurements by Fries et al. [18] The exchange constant (A_{ex}) of Co_2B is assumed to be 1 pJ/m and in the considered range independent of temperature.

In order to calculate ΔS_T, the initial magnetization is set to be random, so that the net magnetization of the sample is zero.

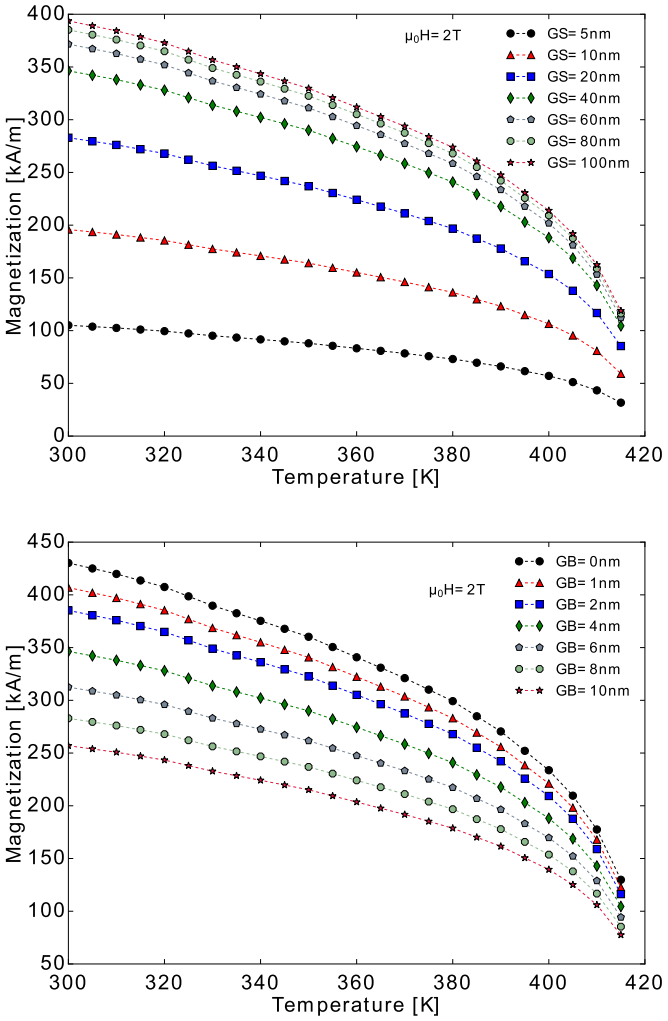

Fig. 1. Simulated magnetization curves for varied grain size with a grain boundary thickness of 4 nm (top) and for varied grain boundary thicknesses with a grain size of 40 nm.

The magnetization process is simulated by applying an external magnetic field in the x-direction, which is parallel to the [100]-direction of the Co_2B grains. For temperatures higher than 100 K, Co_2B exhibits the easy-plane anisotropy, spanned by the [100] and [010] direction. Thus, the magnetic field is applied parallel to an easy axis.

The magnetic field is increased from 0 up to 2 T by increments of 10 mT. As these simulations are isothermal, the same procedure is repeated for temperatures from 300 up to 415 K in increments of 5 K. The Curie temperature (T_C) of Co_2B is 420 K. The magnetization reversal process during the micromagnetic simulation can be seen in Fig. 3 in the supplementary. The resulting magnetization curves are shown in Fig. 1. As expected, the magnetization decreases for smaller grains and thicker grain boundaries. In both cases, the volume ratio of grain to grain boundary decreases, resulting in less magnetic material per unit volume.

In order to calculate ΔS_T we need to extrapolate our micromagnetic simulation results to temperatures above T_C. We apply the Kouvel–Fisher method to obtain a set of β and γ values for each grain size and grain boundary thickness. The trends can be seen in Fig. 2. The largest β and γ values of 0.308 and 1.35, respectively, are obtained for small grains of 5 nm and decrease monotonically towards 0.306 and 1.12. For the variation of grain boundary thickness, β decreases monotonically from 0.307 for 10 nm to

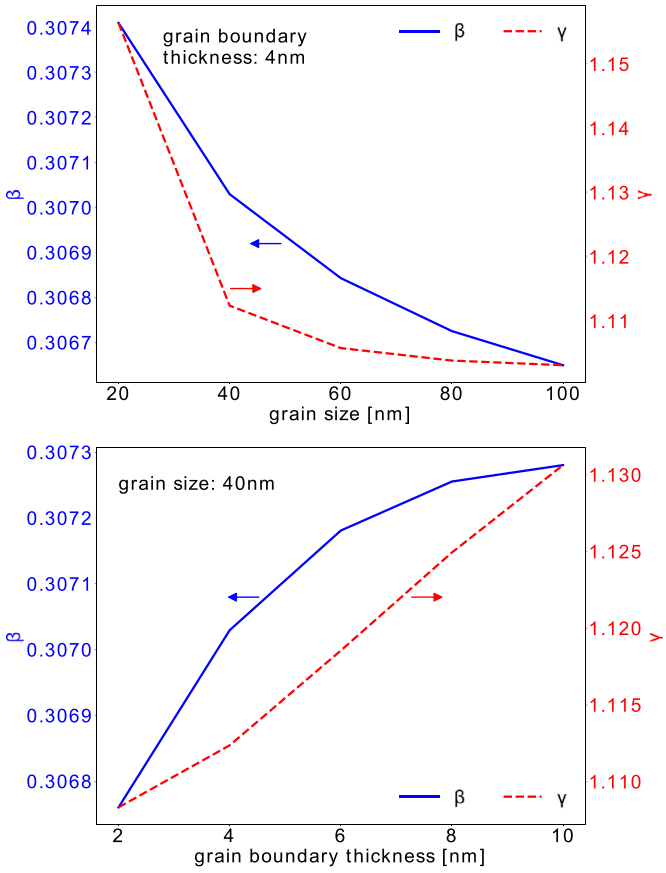

Fig. 2. β and γ as a function of grain size (top) and grain boundary thickness (bottom).

0.305 for 0 nm. γ ranges between 1.12 and 1.15 with a minimum for 1 nm thick grain boundaries. However, for thicker grain boundaries γ increases monotonically. Based on these observations, the size of the grains is expected to have a larger impact on the MCE calculations than the thickness of the grain boundary. Physically, the larger variation of γ implies that the sensitivity of the system to an external field H depends more on the size of the grains. Edge and corner effects are more pronounced in smaller grains, as the surface to volume ratio increases for decreasing grain size.

Inserting the obtained parameters into Eq. (1), ΔS_T can be obtained by the Maxwell relation

$$\Delta S_T = \int_0^{H_{ext}} \left(\frac{\partial M}{\partial T}\right)_H dH\,. \tag{4}$$

ΔS_T as a function of temperature for the different microstructures is shown in Fig. 3. The inset shows the measured entropy change in poly-crystalline Co_2B and in a Co_2B single crystal in an external field of 2 T. [18]

With the assumptions made and the simple microstructures generated, our simulation results agree well with the experimental data. We obtain ΔS_T values between -1.7 and -3.2 Jkg^{-1}K^{-1} at T_C, compared to -1.4 Jkg^{-1}K^{-1} for the single crystal measurement with the external field parallel to the easy axis and -1.2 Jkg^{-1}K^{-1} for the poly-crystalline sample. Larger ΔS_T values are expected as the change of magnetization with temperature in the vicinity of T_C is larger for the ANE curves (see Fig. 2). In addition, the generated microstructures are free of defects and impurities. The magnetization is free to rotate and align with the external field, resulting in larger $\left(\frac{\partial M}{\partial T}\right)_H$ values and thus larger theoretic entropy changes.

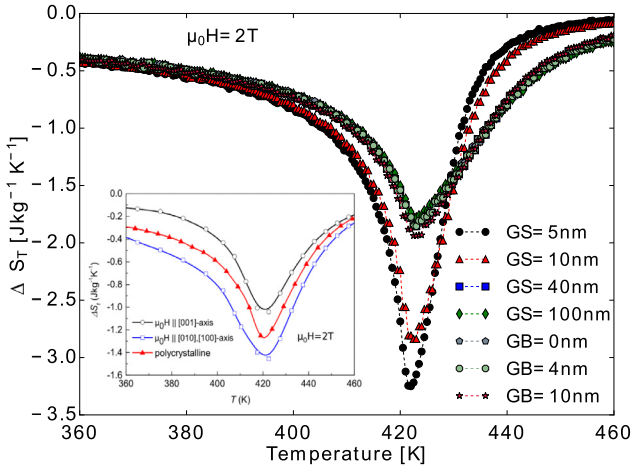

Fig. 3. Specific isothermal entropy change ΔS_T calculated via the ANE as a function of grain size and grain boundary thickness. The inset shows the experimentally measured entropy change in Ref. [18].

Consequently, the calculated ΔS_T curves show a sharper behavior around T_C.

As expected from the obtained γ values, ΔS_T varies only slightly for different grain boundary thicknesses. The largest ΔS_T is found for 10 nm grain boundaries with -1.94 Jkg^{-1}K^{-1}. For smaller boundaries ΔS_T decreases, showing a minimum of -1.82 Jkg^{-1}K^{-1} for 1 nm. This reconciles with the minimum of γ in Fig. 2. We conclude, that the thickness of the non-magnetic grain boundary has only a minor influence on the MCE and is no important parameter for its optimization.

In contrast, the variation of the grain size significantly influences the obtained ΔS_T. For larger grains ΔS_T tends to saturate towards -1.8 Jkg^{-1}K^{-1}, while for smaller grains ΔS_T increases, reaching -3.25 Jkg^{-1}K^{-1} for 5 nm grains. As expected from Fig. 2, the change in ΔS_T is more significant for the variation of grain size than for the variation of boundary thickness. Due to the increased volume to surface ratio, edge and corner effects will be stronger in smaller grains. Therefore, at the same external field the magnetization in smaller grains will be more sensitive to temperature, increasing $\left(\frac{\partial M}{\partial T}\right)_H$. Hence, we speculate that finer microstructures enhance the MCE.

Recent experiments on the relation between the particle size and the MCE showed that ΔS_T decreases with decreasing particle size [37–39]. However, they also reported that the magnetic properties change alongside the particle size change, e.g. smaller M_S values for smaller particles, which results in smaller ΔS_T. In our simulation results in Fig. 3, we only consider ideal grains with the same M_S. However, if we consider the significantly reduced M_S with decreased grain size, we also computationally address that smaller grains lead to smaller ΔS_T values (see Fig. xx in supplementary), consistent with the experimental reports [37–39]. Therefore, with reasonable inputs, our calculation methodology is reliable.

We also calculated ΔS_T for the external magnetic field along the hard axis (see Fig. 4 in supplementary). Consistent with the experimental results, ΔS_T at 2 T is smaller compared to the case with the external magnetic field along the easy axis, as higher fields are required to fully reverse the magnetization along the hard axis and the transition is not so sharp.

Besides investigating the influence of the microstructure on the MCE, our proposed methodology can also be used to examine the influence of magnetocrystalline anisotropy K. That the anisotropy of the system has an influence on the MCE can be seen in the inset of Fig. 3. ΔS_T of a Co_2B single crystal measured in an external

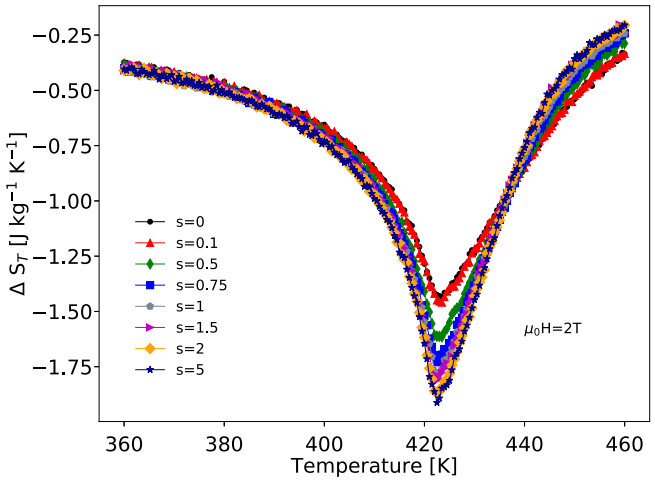

Fig. 4. Comparison of ΔS_T for scaled magnetic anisotropy constants K.

field parallel to the easy axis is 0.4 $Jkg^{-1}K^{-1}$ larger than in a field parallel to the hard axis.

In the same way as for the microstructure variation, we perform micromagnetic simulations up to 415 K for scaled K values that retain the relative temperature dependence. K is scaled with a factor s that ranges from 0 to 5 (see Fig. 4 in supplementary), where 0 corresponds to the isotropic case. We use the Kouvel-Fisher method to obtain β and γ, and calculate ΔS_T using Eqs. (1) and (4). a and b are taken as the same values as before. We are aware that varying an intrinsic property like the magnetocrystalline anisotropy may also influence the parameters a and b. Nevertheless, we are confident to show the principle relation between the magnetocrystalline anisotropy and the MCE. The results for ΔS_T are shown in Fig. 4.

ΔS_T is the lowest for the isotropic case (s=0) and increases with larger scaling factors (i.e. larger K). This is related to the anisotropy energy which linearly depends on K and therefore scales with s. For larger anisotropy energies, the misalignment of magnetic moments with the easy directions costs more energy and the system tends to align faster with the external field. ΔS_T ranges from -1.4 to -1.95 $Jkg^{-1}K^{-1}$ and is found to saturate for larger K, showing almost identical results for s equal to 2 and 5.

In summary, we have proposed a new methodology for calculating MCE in SOPT materials from micromagnetic simulations. We combine mircomagnetic simulations with the ANE to extrapolate the simulation results to temperatures at and above T_C. Experimental data is used to obtain the material-specific parameters a and b of ANE, while the critical exponents β and γ of ANE are determined by using mircomagnetic simulations and the Kouvel-Fisher method. Assuming a and b to be constant for the model material Co_2B, we determined β and γ by using micromagnetic simulations results of different microstructures and anisotropy constants. ΔS_T calculated by our methodology shows good agreement with the experimental results on Co_2B. It is found that ΔS_T increases with decreasing grain size, increasing grain boundary thickness, and increasing K.

Our proposed methodology is supposed to help optimizing the MCE by tuning the microstructure in SOPT materials. We are confident, that our approach can be used to predict the trend of the MCE with respect to the microstructure. This allows for a more systematic synthesis of microstructures with a predicted higher MCE. Our results imply that the MCE can be enhanced by reducing the grain size in poly-crystalline SOPT materials, when the magnetic properties of the grains are not changed by the size reduction. If M_S is significantly reduced by decreasing the grain size, smaller grains could also lead to smaller ΔS_T. In any case, results shown in this work serve as a proof of concept of our new methodology. More extensive calculations with more complex microstructures, including different grain sizes, shapes, and orientations as well as different grain boundary properties have to be performed to gain further insight on the relation between microstructure and the MCE.

Declaration of Competing Interest

The authors declare that they have no known competing financial interests or personal relationships that could have appeared to influence the work reported in this paper.

Acknowledgment

The authors acknowledge the support from the European Research Council (ERC) under the European Unions Horizon 2020 research and innovation programme (Grant agreement No 743116, project CoolInnov), the support from the German Research Foundation (DFG YI 165/1-1 and DFG XU 121/7-1), and the access to the Lichtenberg High Performance Computer of Technische Universität Darmstadt. M Yi acknowledges the support of the 15th Thousand Youth Talents Program of China, the NSFC (Grant No. 11902150), the Research Fund of State Key Laboratory of Mechanics and Control of Mechanical Structures (MCMS-I-0419G01), and A Project Funded by the Priority Academic Program Development of Jiangsu Higher Education Institutions.

Supplementary material

Supplementary material associated with this article can be found, in the online version, at doi:10.1016/j.scriptamat.2019.10.039.

References

[1] C. Zimm, A. Jastrab, A. Sternberg, V. Pecharsky, K. Gschneidner, M. Osborne, I. Anderson, P. Kittel, in: Advances in Cryogenic Engineering, Springer US, Boston, MA, 1998, pp. 1759–1766, doi:10.1007/978-1-4757-9047-4_222.
[2] O. Gutfleisch, M.A. Willard, E. Brück, C.H. Chen, S.G. Sankar, J.P. Liu, Adv. Mater. 23 (7) (2011) 821–842, doi:10.1002/adma.201002180.
[3] V. Franco, J.S. Blázquez, B. Ingale, A. Conde, Annu. Rev. Mater. Res. 42 (1) (2012) 305–342, doi:10.1146/annurev-matsci-062910-100356.
[4] V.K. Pecharsky, K.A. Gschneidner, Phys. Rev. Lett. 78 (23) (1997) 4494–4497, doi:10.1103/PhysRevLett.78.4494.
[5] F.X. Hu, B.G. Shen, J.R. Sun, Z.H. Cheng, G.H. Rao, X.X. Zhang, Appl. Phys. Lett. 78 (23) (2001) 3675–3677, doi:10.1063/1.1375836.
[6] A. Fujita, S. Fujieda, Y. Hasegawa, K. Fukamichi, Phys. Rev. B – Condens. Matter Mater. Phys. 67 (10) (2003) 12, doi:10.1103/PhysRevB.67.104416.
[7] J. Lyubina, R. Schäfer, N. Martin, L. Schultz, O. Gutfleisch, Adv. Mater. 22 (33) (2010) 3735–3739, doi:10.1002/adma.201000177.
[8] J. Liu, J.D. Moore, K.P. Skokov, M. Krautz, K. Löwe, A. Barcza, M. Katter, O. Gutfleisch, Scr. Mater. 67 (6) (2012) 584–589, doi:10.1016/j.scriptamat.2012.05.039.
[9] O. Tegus, E. Brueck, K.H.J. Buschow, F.R. de Boer, Nature 415 (2002) 150, doi:10.1002/chin.200214015.
[10] A. Yan, K.H. Müller, L. Schultz, O. Gutfleisch, J. Appl. Phys. 99 (8) (2006) 0–4, doi:10.1063/1.2162807.
[11] F. Guillou, G. Porcari, H. Yibole, N. Van Dijk, E. Brück, Adv. Mater. 26 (17) (2014) 2671–2675, doi:10.1002/adma.201304788.
[12] M. Fries, L. Pfeuffer, E. Bruder, T. Gottschall, S. Ener, L.V.B. Diop, T. Gröb, K.P. Skokov, O. Gutfleisch, Acta Mater. 132 (2017) 222–229, doi:10.1016/j.actamat.2017.04.040. URL: http://www.sciencedirect.com/science/article/pii/S1359645417303348
[13] J. Liu, T. Gottschall, K.P. Skokov, J.D. Moore, O. Gutfleisch, Nat. Mater. 11 (7) (2012) 620–626, doi:10.1038/nmat3334.
[14] T. Gottschall, K.P. Skokov, D. Benke, M.E. Gruner, O. Gutfleisch, Phys. Rev. B 93 (18) (2016) 2–7, doi:10.1103/PhysRevB.93.184431.
[15] J.Y. Law, V. Franco, L.M. Moreno-Ramírez, A. Conde, D.Y. Karpenkov, I. Radulov, K.P. Skokov, O. Gutfleisch, Nat. Commun. 9 (1) (2018) 2680, doi:10.1038/s41467-018-05111-w.
[16] J. Liu, M. Krautz, K. Skokov, T.G. Woodcock, O. Gutfleisch, Acta Mater. 59 (9) (2011) 3602–3611, doi:10.1016/j.actamat.2011.02.033.
[17] T. Gottschall, D. Benke, M. Fries, A. Taubel, I.A. Radulov, K.P. Skokov, O. Gutfleisch, Adv. Funct. Mater. 27 (32) (2017) 1–6, doi:10.1002/adfm.201606735.

[18] M. Fries, K.P. Skokov, D.Y. Karpenkov, V. Franco, S. Ener, O. Gutfleisch, Appl. Phys. Lett. 109 (23) (2016) 232406, doi:10.1063/1.4971839.
[19] B.N. Harmon, V.N. Antonov, J. Appl. Phys. 91 (12) (2002) 9815–9820, doi:10.1063/1.1461896.
[20] D. Paudyal, V.K. Pecharsky, K.A. Gschneidner, B.N. Harmon, Phys. Rev. B 73 (144406) (2006) 1–12, doi:10.1103/PhysRevB.74.012403.
[21] V.D. Buchelnikov, V.V. Sokolovskiy, H.C. Herper, H. Ebert, M.E. Gruner, S.V. Taskaev, V.V. Khovaylo, A. Hucht, A. Dannenberg, M. Ogura, H. Akai, M. Acet, P. Entel, Phys. Rev. B 81 (9) (2010) 094411, doi:10.1103/PhysRevB.81.094411.
[22] C.P. Bean, D.S. Rodbell, Phys. Rev. 126 (1) (1962) 104–115, doi:10.1103/PhysRev.126.104.
[23] V. Basso, G. Bertotti, M. Lobue, C.P. Sasso, J. Magn. Magn. Mater. 290–291 PA (2005) 654–657, doi:10.1016/j.jmmm.2004.11.324.
[24] Y.I. Spichkin, A.M. Tishin, J. Magn. Magn. Mater. 290–291 PA (2005) 700–702, doi:10.1016/j.jmmm.2004.11.341.
[25] H. Oesterreicher, F.T. Parker, J. Appl. Phys. 55 (12) (1984) 4334–4338, doi:10.1063/1.333046.
[26] A.Y. Romanov, V.P. Silin, Fiz. Metall. Metall. 83 (2) (1997) 5–11.
[27] V. Franco, A. Conde, L.F. Kiss, J. Appl. Phys. 104 (3) (2008) 1–5, doi:10.1063/1.2961310.
[28] A. Arrott, J.E. Noakes, Phys. Rev. Lett. 19 (14) (1967) 786–789, doi:10.1103/PhysRevLett.19.786.
[29] D.C. Crew, E. Girt, D. Suess, T. Schrefl, K.M. Krishnan, G. Thomas, M. Guilot, Phys. Rev. B – Condens. Matter Mater. Phys. 66 (18) (2002) 1–13, doi:10.1103/PhysRevB.66.184418.
[30] A. Thiaville, J.M. García, R. Dittrich, J. Miltat, T. Schrefl, Phys. Rev. B – Condens. Matter Mater. Phys. 67 (9) (2003) 1–12, doi:10.1103/PhysRevB.67.094410.
[31] M. Yi, O. Gutfleisch, B.X. Xu, J. Appl. Phys. 120 (3) (2016), doi:10.1063/1.4958697.
[32] J.C. Maxwell, P. Trans, R.S. Lond, Philos. Trans. R. Soc. Lond. 155 (January) (1865) 459–512, doi:10.1098/rstl.1865.0008.
[33] J.S. Kouvel, M.E. Fisher, Phys. Rev. 136 (6A) (1964), doi:10.1103/PhysRev.136.A1626.
[34] C. Domb, M.F. Sykes, Phys. Rev. 128 (1) (1962) 168–173, doi:10.1103/PhysRev.128.168.
[35] C. Domb, M.F. Sykes, J. Math. Phys. 2 (1) (1961) 63–67, doi:10.1063/1.1724213.
[36] M. Donahue, D. Porter, J. Lau, R. McMichael, NIST J. Res. 114 (1999) 57–67.
[37] T. Toliński, K. Synoradzki, Acta Phys. Pol. A 126 (1) (2014) 160–161, doi:10.12693/APhysPolA.126.160.
[38] M. Kaya, I. Dincer, S. Akturk, Y. Elerman, Metall. Mater. Trans. A: Phys. Metall. Mater. Sci. 47 (10) (2016) 4983–4987, doi:10.1007/s11661-016-3661-x.
[39] H. Baaziz, A. Tozri, E. Dhahri, E.K. Hlil, Chem. Phys. Lett. 691 (2018) 355–359, doi:10.1016/j.cplett.2017.10.021.